Computer Assisted Mechanics and Engineering Sciences, 3: 233–243, 1996.

Natural vibration frequencies of delaminated composite beams

Marek Krawczuk, Wiesław Ostachowicz and Arkadiusz Żak
Institute of Fluid Flow Machinery, Polish Academy of Sciences,
80–952 Gdańsk, ul. Gen. J. Fiszera 14, Poland

(Received August 9, 1995)

In the presented work a model of a layered, delaminated composite beam based on the finite elements method was introduced. In this model the beam was divided into finite elements, while the delamination was modelled using additional boundary conditions. One delaminated region in the cross-section of the beam was considered which extended to the full width of the beam. It was also assumed that the delamination was open. The influence of the delamination length and position on the changes of natural frequencies of flexural vibrations of the laminated composite cantilever beam were investigated.

1. Introduction

Recent years have brought a considerable growth in the applications of anisotropic reinforced laminated composites in the field of mechanical and civil engineering. Nowadays these materials are widely used in modern high-speed machinery and lightweight structures where high strength-to-weight ratios are required.

Delamination is one of the most important failure modes in laminated composite materials. Acquired during the manufacturing process or produced by impact and other service hazards, delamination may greatly reduce the stiffness of the whole structure, thus influencing the vibration and stability characteristics.

The influence of delamination on the buckling and post-buckling deformation and the delamination growth with different geometrical parameters, loading conditions, material properties and boundary conditions have been studied extensively in the past [1, 2, 3, 10, 14]. Only a few efforts have been made to study the effect of delamination on the vibration characteristics. Natural vibrations of delaminated beams have been studied by Ramkumar [6] on the basis of the Timoshenko beam theory. The authors did not, however, take into account the effect of coupling of the transverse vibration with the longitudinal wave motion in the upper and lower split layers. The analytical results obtained by them predicted significant reduction of the fundamental frequency, and this prediction did not agree with their experimental observation. Wang et al. [9] applied the classical beam theory but, contrary to Ramkumar [6], they considered the coupling effect. In case of including the coupling effects, the calculated fundamental frequency was not sufficiently reduced by the presence of a relatively short delamination and the results were in close agreement with experimental measurements. Woźniak et. al. studied the influence of micro-cracks densities on the material properties in the macro scale [11], and also investigated the effects of interlaminar imperfections on behaviour of composite shells [12, 13]. Natural frequencies of a composite beam with delamination originating from a transverse crack have been analysed by Ostachowicz and Krawczuk [5].

The present work is devoted to the analysis of natural vibrations of a layered composite beam with a single delamination. The beam is modelled by finite beam elements with three nodes and three degrees of freedom at each node (i.e., the transverse and axial displacements and the in-

dependent rotation). In the delaminated region, additional boundary conditions are applied. It is assumed that the delamination is open (i.e., damping caused by contact forces between lower and upper parts can be neglected in the model due to its small influence on changes of natural frequencies) and extends to the full width of the beam. The influence of the delamination length and position on the changes of natural flexural frequencies of the laminated composite cantilever beam is investigated.

2. Formulation of a delamination model

In Fig. 1, a model of a delaminated part of the beam is presented. The delaminated region is modelled by three finite beam elements which are connected at the delamination crack tip where additional boundary conditions are applied.

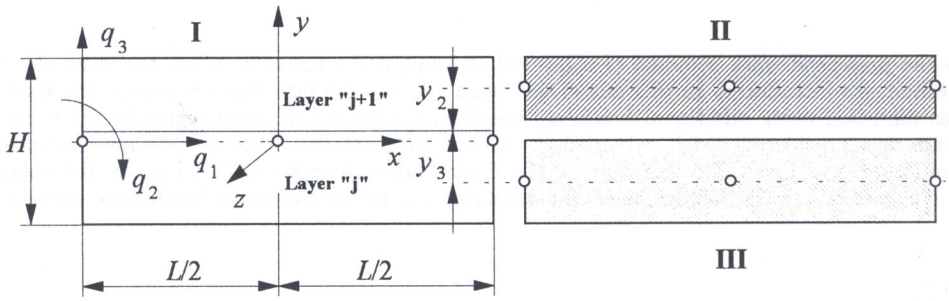

Fig. 1. Delamination of a beam modelled by finite elements

The layers are located symmetrically with respect to the x-z plane. Each element has three nodes ($x = -L/2$, $x = 0$, $x = L/2$) with three degrees of freedom, which are axial displacements q_i ($i = 1, 4, 7$), transverse displacements q_i ($i = 3, 6, 9$) and the independent rotations q_i ($i = 2, 5, 8$). It is also assumed that the number of degrees of freedom is independent of the number of layers.

2.1. Description of the element No. I

Neglecting the effect of warping, the axial displacements u and v of a point can be expressed as:

$$\begin{cases} u(x,y) = u^0(x) - y\phi(x)\,, \\ \nu(x,y) = \nu^0(x) \end{cases} \tag{1}$$

where $u^0(x)$ denotes the axial displacement, $\phi(x)$ — the independent rotation, and $\nu^0(x)$ — the transverse displacement.

The bending displacement $\nu^0(x)$ is assumed to be a cubic polynomial in x, while the axial displacement $u^0(x)$ and the rotation $\phi(x)$ are assumed to be quadratic functions of x. Additionally it is assumed that the shear strain variation is linear [7]. Applying the above conditions, the displacements and rotation in the element may be written in the following form:

$$\begin{cases} u^0(x) = a_1 + a_2 x + a_3 x^2\,, \\ \phi(x) \;\; = a_4 + a_5 x + 3a_9 x^2\,, \\ \nu^0(x) = a_6 + a_7 x + a_8 x^2 + a_9 x^3\,. \end{cases} \tag{2}$$

The constants $a_1 - a_9$ can be expressed in terms of the degrees of freedom of the element by using the nodal conditions in the following form:

$$\begin{cases} u^0(x=-L/2) = q_1\,, \\ \phi(x=-L/2) \;\; = q_2\,, \\ \nu^0(x=-L/2) = q_3\,, \end{cases} \quad \begin{cases} u^0(x=0) = q_4\,, \\ \phi(x=0) \;\; = q_5\,, \\ \nu^0(x=0) = q_6\,, \end{cases} \quad \begin{cases} u^0(x=L/2) = q_7\,, \\ \phi(x=L/2) \;\; = q_8\,, \\ \nu^0(x=L/2) = q_9\,. \end{cases} \tag{3}$$

Finally we obtain:

$$\begin{cases} a_1 = q_4\,, \\ a_3 = (q_7 - q_1)/L\,, \\ a_3 = 2(q_1 - 2q_4 + q_7)/L^2\,, \\ a_4 = q_6\,, \\ a_5 = (q_9 - q_3)/L\,, \\ a_6 = q_5\,, \\ a_7 = (2q_6 L + 6q_8 - 6q_2 - q_3 L - q_9 L)/6L\,, \\ a_8 = 2(q_2 - 2q_5 + q_8)/L^2\,, \\ a_9 = 2(q_3 - 2q_6 + q_9)/3L^2\,. \end{cases} \tag{4}$$

Taking into account Eqs. (4) and Eq. (2), the matrix of the shape function for a single layer of the element can be determined,

$$\mathbf{N} = \mathbf{X}\mathbf{A} \tag{5}$$

where matrix $\mathbf{X}$ has the form:

$$\mathbf{X} = \begin{bmatrix} 1 & x & x^2 & -y & -xy & 0 & 0 & 0 & -3x^2 y \\ 0 & 0 & 0 & 0 & 0 & 1 & x & x^2 & x^3 \end{bmatrix}, \tag{6}$$

whereas the matrix $\mathbf{A}$ can be expressed by:

$$\mathbf{A} = \begin{bmatrix} 0 & 0 & 0 & 1 & 0 & 0 & 0 & 0 & 0 \\ -\frac{1}{L} & 0 & 0 & 0 & 0 & 0 & \frac{1}{L} & 0 & 0 \\ \frac{2}{L^2} & 0 & 0 & -\frac{4}{L^2} & 0 & 0 & \frac{2}{L^2} & 0 & 0 \\ 0 & 0 & 0 & 0 & 0 & 1 & 0 & 0 & 0 \\ 0 & 0 & -\frac{1}{L} & 0 & 0 & 0 & 0 & 0 & \frac{1}{L} \\ 0 & 0 & 0 & 0 & 1 & 0 & 0 & 0 & 0 \\ 0 & -\frac{1}{L} & -\frac{1}{6} & 0 & 0 & \frac{1}{3} & 0 & \frac{1}{L} & -\frac{1}{6} \\ 0 & \frac{2}{L^2} & 0 & 0 & -\frac{4}{L^2} & 0 & 0 & \frac{2}{L^2} & 0 \\ 0 & 0 & \frac{2}{3L^2} & 0 & 0 & -\frac{4}{3L^2} & 0 & 0 & \frac{2}{3L^2} \end{bmatrix}. \tag{7}$$

Using the shape function matrix for a single layer, the inertia matrix of the whole element can be calculated from the formula

$$\mathbf{M}^{\mathrm{e}} = \sum_{j=1}^{R} \mathbf{M}_j^{\mathrm{e}} = \sum_{j=1}^{R} \rho_j \int_{V_j} \mathbf{N}^{\mathrm{T}}\mathbf{N}\,\mathrm{d}V_j = \sum_{j=1}^{R} \rho_j \mathbf{A}^{\mathrm{T}} \int_{V_j} \mathbf{X}^{\mathrm{T}}\mathbf{X}\,\mathrm{d}V_j\,\mathbf{A} = \sum_{j=1}^{R} \rho_j \mathbf{A}^{\mathrm{T}} \tilde{\mathbf{M}}_j^{\mathrm{e}} \mathbf{A}\,, \tag{8}$$

where j denotes the number of the layer, R — the total number of layers in the element, V_j — the volume of the j-th layer of material and ρ_j — the density of the j-th layer.

The value of the integral in Eq. (8) (for the j-th layer) can be expressed in the closed form,

$$\mathbf{M}_j^{\mathrm{e}} = BL \begin{bmatrix} \alpha & 0 & \frac{L^2}{12}\alpha & -\frac{1}{2}\beta & 0 & 0 & 0 & 0 & -\frac{L^2}{8}\beta \\ & \frac{L^2}{12}\alpha & 0 & 0 & -\frac{L^2}{24}\beta & 0 & 0 & 0 & 0 \\ & & \frac{L^4}{80}\alpha & -\frac{L^2}{24}\beta & 0 & 0 & 0 & 0 & -\frac{3L^4}{160}\beta \\ & & & \frac{1}{3}\gamma & 0 & 1 & 0 & 0 & \frac{L^2}{12}\gamma \\ & & & & \frac{L^2}{36}\gamma & 0 & 0 & 0 & 0 \\ & & & & & \alpha & 0 & \frac{L^2}{12}\alpha & 0 \\ & & & & & & \frac{L^2}{12}\alpha & 0 & \frac{L^4}{80}\alpha \\ & \text{symm.} & & & & & & \frac{L^4}{80}\alpha & 0 \\ & & & & & & & & \frac{L^6}{448}\alpha + \frac{3L^4}{80}\gamma \end{bmatrix}, \tag{9}$$

where $\alpha = H_{j+1} - H_j$, $\beta = H_{j+1}^2 - H_j^2$, $\gamma = H_{j+1}^3 - H_j^3$.

The strains in a single layer of the material are given by the following formulas:

$$\begin{cases} \varepsilon_x &= \dfrac{\partial u(x,y)}{\partial x} = \dfrac{\partial u^0(x)}{\partial x} - y\dfrac{\partial \phi(x)}{\partial x}\,, \\ \gamma_{xy} &= \dfrac{\partial u(x,y)}{\partial y} + \dfrac{\partial \nu(x,y)}{\partial x} = \dfrac{\partial \nu^0(x)}{\partial x} - \phi(x)\,. \end{cases} \tag{10}$$

Considering relations (2) and (4), the strains in the single layer can be expressed as a function of nodal degrees of freedom:

$$\begin{Bmatrix} \varepsilon_x \\ \gamma_{xy} \end{Bmatrix} = \mathbf{B} \begin{Bmatrix} q_1 \\ q_2 \\ \vdots \\ q_9 \end{Bmatrix}, \tag{11}$$

where the matrix $\mathbf{B}$ equals

$$\mathbf{B} = \tilde{\mathbf{X}}\mathbf{A} \tag{12}$$

while the matrix $\tilde{\mathbf{X}}$ is given by

$$\tilde{\mathbf{X}} = \begin{bmatrix} 0 & 1 & 2x & 0 & -y & 0 & 0 & 0 & -6xy \\ 0 & 0 & 0 & -1 & -x & 0 & 1 & 2x & 0 \end{bmatrix}. \tag{13}$$

The stiffness matrix of the whole element can be calculated from the following equation:

$$\mathbf{K}^{\mathrm{e}} = \sum_{j=1}^{R} \mathbf{K}_j^{\mathrm{e}} = \sum_{j=1}^{R} \int_{V_j} \mathbf{B}^{\mathrm{T}} \mathbf{D}_j \mathbf{B} \, \mathrm{d}V_j = \sum_{j=1}^{R} \mathbf{A}^{\mathrm{T}} \int_{V_j} \tilde{\mathbf{X}}^{\mathrm{T}} \mathbf{D}_j \tilde{\mathbf{X}} \, \mathrm{d}V_j \, \mathbf{A} = \sum_{j=1}^{R} \mathbf{A}^{\mathrm{T}} \tilde{\mathbf{K}}_j^{\mathrm{e}} \mathbf{A} \,, \tag{14}$$

where $\mathbf{D}_j$ denotes the matrix which describes the relations between stresses and strains in the j-th layer of the element (see Appendix A).

The value of the integral in Eq. (14) (for the j-th layer of the material) can be presented in closed form,

$$\mathbf{K}_j^{\mathrm{e}} = BL \begin{bmatrix} 0 & 0 & 0 & 0 & 0 & 0 & 0 & 0 & 0 \\ & S_{11}\alpha & 0 & -S_{16}\alpha & -\frac{S_{11}}{2}\beta & 0 & S_{16}\alpha & 0 & 0 \\ & & \frac{S_{11}L^2}{3}\alpha & 0 & -\frac{S_{16}L^2}{6}\alpha & 0 & 0 & \frac{S_{16}L^2}{6}\alpha & -\frac{S_{11}L^2}{2}\beta \\ & & & S_{66}\alpha & \frac{S_{16}}{2}\beta & 0 & -S_{66}\alpha & 0 & 0 \\ & & & & \frac{S_{66}L^2\alpha + 4S_{11}\gamma}{12} & 0 & -\frac{S_{66}L^2}{6}\alpha & -\frac{S_{66}L^2}{6}\alpha & 0 \\ & & & & & 0 & 0 & 0 & 0 \\ & & & & & & S_{66}\alpha & 0 & 0 \\ & & & & & & & \frac{S_{66}L^2}{3}\alpha & -\frac{S_{16}L^2}{2}\beta \\ & \text{symm.} & & & & & & & S_{11}\gamma \end{bmatrix}, \tag{15}$$

where $\alpha = H_{j+1} - H_j$, $\beta = H_{j+1}^2 - H_j^2$, $\gamma = H_{j+1}^3 - H_j^3$.

2.2. Description of elements Nos. II and III

In order to connect element I with elements II and III, the following boundary conditions are applied at the delamination crack tip:

$$\begin{cases} \phi_1(x) = \phi_2(x) = \phi_3(x) \,, \\ \nu_1^0(x) = \nu_2^0(x) = \nu_3^0(x) \,, \end{cases} \qquad \begin{cases} u_1^0(x) - y_2\phi_2(x) = u_2^0(x) \,, \\ u_1^0(x) - y_3\phi_3(x) = u_3^0(x) \,, \end{cases} \tag{16}$$

where y_2 and y_3 denote distances between the neutral axes of elements I–II and I–III, respectively (see Fig. 1).

Taking into account relations (16) and (2), the relationships between constants a_1–a_9 for the elements mentioned above can be evaluated in the form

$$\begin{cases} a_1^{II} = a_1^I - y_2 a_4^I \,, & a_1^{III} = a_1^I - y_3 a_4^I \,, \\ a_2^{II} = a_2^I - y_2 a_5^I \,, & a_2^{III} = a_2^I - y_3 a_5^I \,, \\ a_3^{II} = a_3^I - 3y_2 a_9^I \,, & a_3^{III} = a_3^I - 3y_3 a_9^I \,, \\ a_4^I = a_4^{II} = a_4^{III} \,, & a_7^I = a_7^{II} = a_7^{III} \,, \\ a_5^I = a_5^{II} = a_5^{III} \,, & a_8^I = a_8^{II} = a_8^{III} \,, \\ a_6^I = a_6^{II} = a_6^{III} \,, & a_9^I = a_9^{II} = a_9^{III} \,, \end{cases} \tag{17}$$

where the superscripts I, II and III denote the number of the element in the region of delamination.

The shape function matrices for the elements No. II and III will have the following forms:

$$\mathbf{N}_2 = \mathbf{X}\mathbf{A}_2\,, \tag{18}$$

$$\mathbf{N}_3 = \mathbf{X}\mathbf{A}_3\,, \tag{19}$$

where $\mathbf{A}_i$ $(i = 1, 2)$ is given by the following formula

$$\mathbf{A}_i = \begin{bmatrix} 0 & 0 & 0 & 1 & 0 & y_i & 0 & 0 & 0 \\ -\frac{1}{L} & 0 & \frac{y_i}{L} & 0 & 0 & 0 & \frac{1}{L} & 0 & -\frac{y_i}{L} \\ \frac{2}{L^2} & 0 & -\frac{2y_i}{L^2} & -\frac{4}{L^2} & 0 & \frac{4y_i}{L^2} & \frac{2}{L^2} & 0 & -\frac{2y_i}{L^2} \\ 0 & 0 & 0 & 0 & 0 & 1 & 0 & 0 & 0 \\ 0 & 0 & -\frac{1}{L} & 0 & 0 & 0 & 0 & 0 & \frac{1}{L} \\ 0 & 0 & 0 & 0 & 1 & 0 & 0 & 0 & 0 \\ 0 & -\frac{1}{L} & -\frac{1}{6} & 0 & 0 & \frac{1}{3} & 0 & \frac{1}{L} & -\frac{1}{6} \\ 0 & \frac{2}{L^2} & 0 & 0 & -\frac{4}{L^2} & 0 & 0 & \frac{2}{L^2} & 0 \\ 0 & 0 & \frac{2}{3L^2} & 0 & 0 & -\frac{4}{3L^2} & 0 & 0 & \frac{2}{3L^2} \end{bmatrix}. \tag{20}$$

The inertia matrices of elements II and III can be calculated by considering $\mathbf{A}_2$, $\mathbf{A}_3$ and using Eq. (8).

In a similar way, matrices $\mathbf{B}_2$ and $\mathbf{B}_3$ of elements II and III can be evaluated, and finally the stiffness matrices of these elements can be determined, Eq. (14) being used.

3. Numerical calculations

Numerical calculations have been carried out for the cantilever composite beam of the following dimensions: length 600 mm, height 25 mm and width 50 mm (see Fig. 2). The beam was made of a

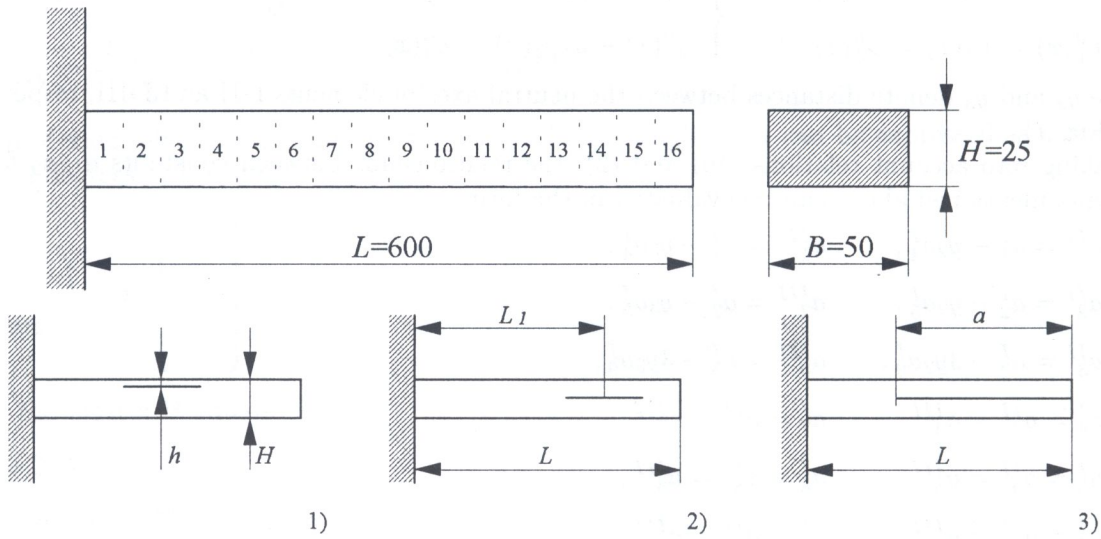

Fig. 2. Geometry of the cantilever composite beam subject to the effects of delamination: 1) location across the beam, 2) location along the beam, 3) total length

graphite-epoxy composite. It was assumed that in all layers of the beam the fibres were inclined at the same angle to the x-axis. The mechanical properties of the material are given in Appendix B.

The first example illustrates the influence of the position of delamination measured across the beam on the changes of the first natural bending vibration frequency for four different volume fractions of the fibres. The length of delamination was equal to 37.5 mm ($a/L = 0.0625$) and the centre of delamination was located 431.25 mm from the free end of the beam ($L_1/L = 0.71875$). The angle of inclination of the fibres (measured from the x-axis of the beam in the x-z plane) was 45 degrees, whereas the volume of fibres was equal to: 20%, 40%, 60% and 80% of the volume of the beam. In this case the beam was modelled by 17 finite elements (2 elements in the layers modelling delamination and 15 elements outside the delaminated region). The results of numerical calculations are given in Fig. 3. It is clearly shown that the largest reduction of the natural frequency is observed when the delamination is located along the neutral axis of the beam. When the delamination is located near the upper or lower surfaces of the beam, the changes of the natural frequencies are negligible.

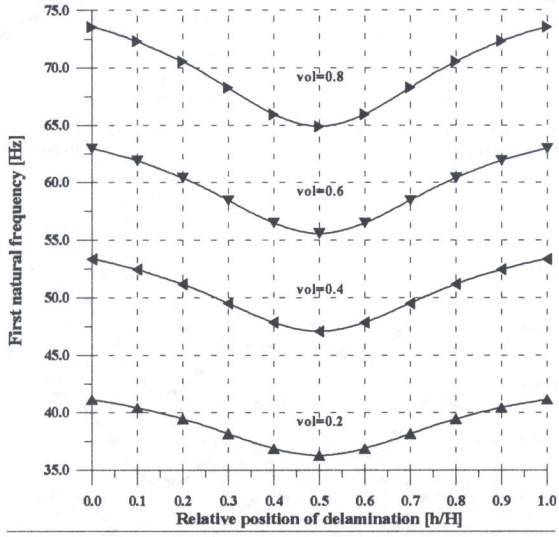

Fig. 3. Effect of the position of delamination measured across the beam upon the first natural bending vibration frequency

The next example shows the influence of the position of delamination measured along the beam on the changes of first three natural vibration frequencies. As in the first and second examples, the beam was made of graphite-epoxy composite material. The delamination was located along the neutral axis of the beam. The length of the delamination was equal to 37.5 mm ($a/L = 0.0625$). In the finite elements modelling, the same number of elements were used as in the first example. Fig. 5 illustrates the influence of location of the delamination for the analysed frequencies of the beam. It is clearly shown that the changes of natural frequencies strongly depend on the location of delamination. For the analysed beam, the largest reduction of the natural frequency is observed if the centre of the delamination is located at the node of the mode shape associated with this frequency.

The third example presents the influence of the length of delamination on the behaviour of the first three natural vibration frequencies. The delamination was located along the neutral axis of the beam and expanded towards the fixed end of the beam. Other parameters were the same as in the first example. To model the growth of the delamination various numbers of finite elements were used (16 in the case of the undelaminated beam and 31 for the maximum delamination length considered). The results of numerical calculations are presented in Fig. 4. It is noted that when the length of the delamination increases, the values of natural frequencies are greatly reduced. The intensity of these changes depends also on the number of the natural frequency (i.e., the mode

shape and the location of delamination along the beam) and volume fraction of the fibres. The reduction of natural frequency increases in the case when volume fraction of the fibres grows.

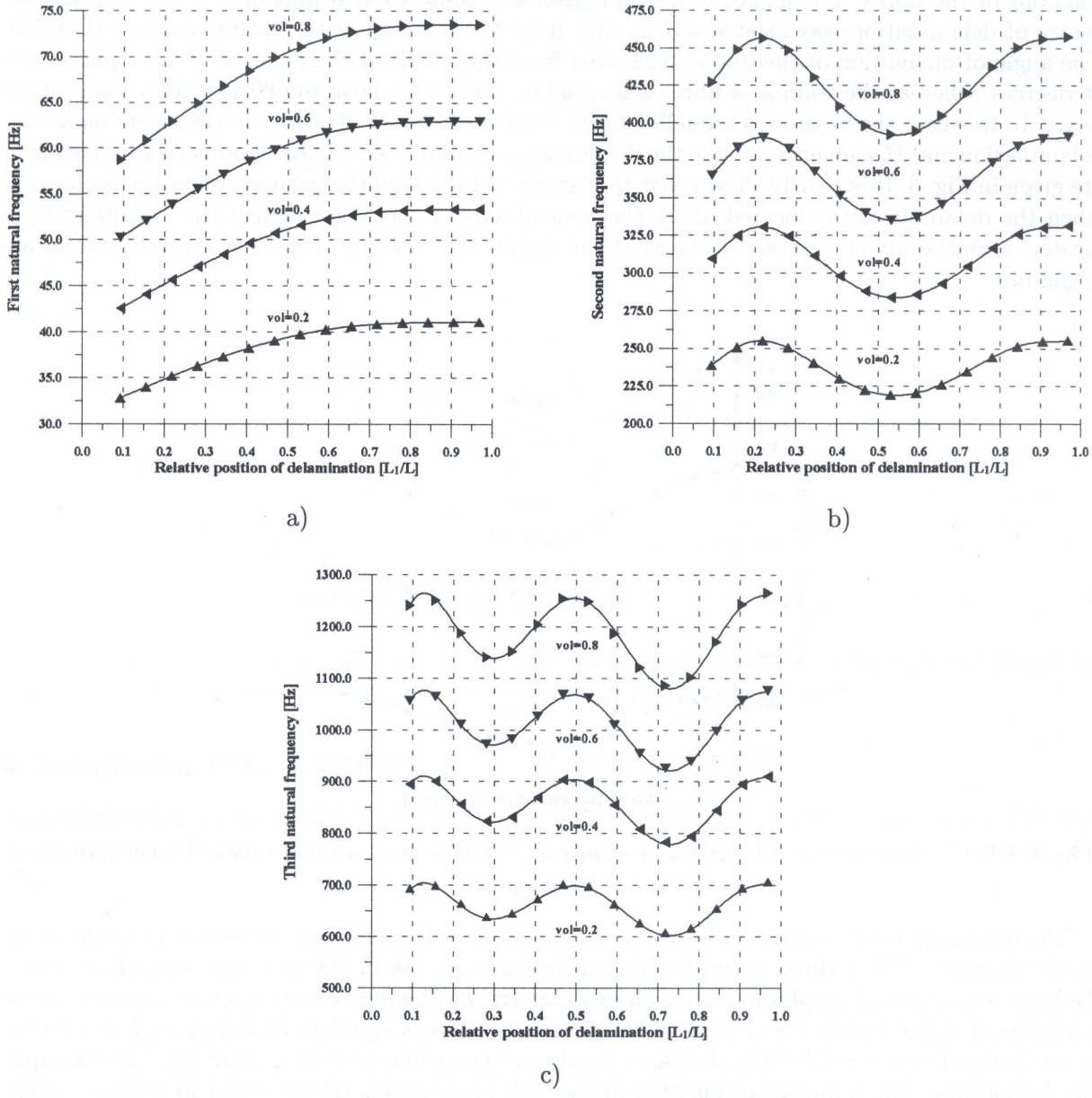

Fig. 4. The effect of the delamination location on the: a) first, b) second, c) third natural bending vibration frequency

4. Conclusions

A model based on finite element was developed to study the natural bending vibration frequencies of a cantilever composite beam with delamination. The method of modelling the delamination in the beam is versatile and allows for the analysis of the influence of multiple delaminations on natural vibration frequencies of beams with various boundary conditions. Using the proposed model, the effects of location and size of the delamination on natural vibration frequencies of the composite beam were studied.

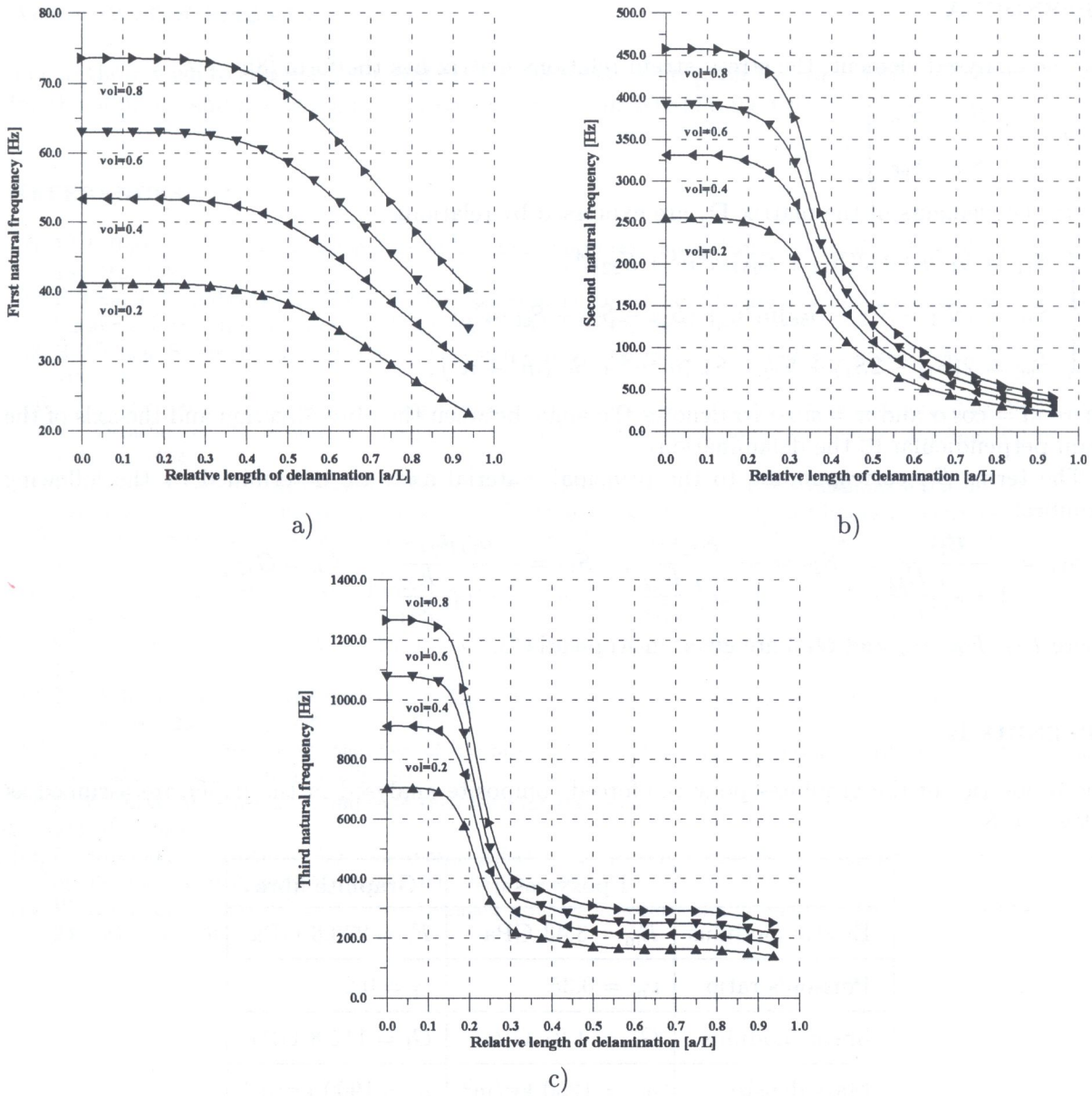

Fig. 5. Influence of the total length of delamination on the: a) first, b) second, c) third natural bending vibration frequency

The numerical investigations carried out allow to draw the following conclusions:

1) In all considered cases the delamination reduces the natural vibration frequencies of the examined composite beam.

2) The changes of natural frequencies are a function of the position of delamination (measured not only along but also across the beam), of the delamination length and of the volume fraction of fibres.

3) The greatest reduction of the natural frequency associated with the analysed mode shape is observed if the centre of delamination is located at the point of maximum bending moment.

4) Reduction of the natural frequencies depends on the location and the length of delamination. It is observed that the greatest reduction appears when the delamination is located along the neutral axis of the beam or when the length of the delamination increases.

APPENDIX A

For the analysed element, the stress–strain relations matrix has the form [8]:

$$\mathbf{D}_j = \begin{bmatrix} \bar{S}_{11} & \bar{S}_{16} \\ \bar{S}_{16} & \bar{S}_{66} \end{bmatrix},$$

where the elements of the matrix $\mathbf{D}_j$ are expressed by relations:

$$\begin{cases} \bar{S}_{11} = S_{11}m^4 + 2(S_{12} + S_{66})m^2n^2 + S_{22}n^4, \\ \bar{S}_{16} = (S_{11} - S_{12} - S_{66})m^3n + (S_{12} - S_{22} + S_{66})n^3m, \\ \bar{S}_{66} = 2(S_{11} - 2S_{12} + S_{22} - S_{66})m^2n^2 + S_{66}(m^4 + n^4), \end{cases}$$

where $m = \cos\alpha$ and $n = \sin\alpha$ (α denotes the angle between the fibre direction and the axis of the beam perpendicular to the delamination).

The terms S_{ij} corresponding to the principal material axes are determined by the following formulas:

$$S_{11} = \frac{E_{11}}{1 - \nu_{12}^2 \dfrac{E_{22}}{E_{11}}}, \quad S_{22} = \frac{E_{22}}{1 - \nu_{12}^2 \dfrac{E_{22}}{E_{11}}}, \quad S_{12} = \frac{\nu_{12}E_{22}}{1 - \nu_{12}^2 \dfrac{E_{22}}{E_{11}}}, \quad S_{66} = G_{12},$$

where E_{11}, E_{22}, ν_{12} and G_{12}, are given in Appendix B.

APPENDIX B

The properties of the graphite-epoxy reinforced composite analysed in the paper are assumed as follows [4, 8]:

	Epoxy resin	Graphite fibre
Elastic modulus	$E_{\mathrm{m}} = 3.43$ GPa	$E_{\mathrm{f}} = 275.6$ GPa
Poisson's ratio	$\nu_{\mathrm{m}} = 0.35$	$\nu_{\mathrm{f}} = 0.2$
Shear modulus	$G_{\mathrm{m}} = 1.27$ GPa	$G_{\mathrm{f}} = 114.8$ GPa
Mass density	$\rho_{\mathrm{m}} = 1250$ kg/m^3	$\rho_{\mathrm{f}} = 1900$ kg/m^3

The material is assumed to be orthotropic with respect to its symmetry axes directed along and perpendicular to the fibres. The gross mechanical properties of the composite are calculated using the following formulas:

$$\begin{aligned} \rho &= \rho_{\mathrm{f}}\, vol + \rho_{\mathrm{m}}(1 - vol), \\ E_{11} &= E_{\mathrm{f}}\, vol + E_{\mathrm{m}}(1 - vol), \\ \nu_{12} &= \nu_{\mathrm{f}}\, vol + \nu_{\mathrm{m}}(1 - vol), \\ E_{22} &= E_{\mathrm{m}} \left[\frac{E_{\mathrm{f}} + E_{\mathrm{m}} + (E_{\mathrm{f}} - E_{\mathrm{m}})\, vol}{E_{\mathrm{f}} + E_{\mathrm{m}} - (E_{\mathrm{f}} - E_{\mathrm{m}})\, vol} \right], \\ G_{12} &= G_{\mathrm{m}} \left[\frac{G_{\mathrm{f}} + G_{\mathrm{m}} + (G_{\mathrm{f}} - G_{\mathrm{m}})\, vol}{G_{\mathrm{f}} + G_{\mathrm{m}} - (G_{\mathrm{f}} - G_{\mathrm{m}})\, vol} \right], \end{aligned}$$

where *vol* denotes the volume fraction of the fibre. The principal axes 1 and 2 lie in the plane of the composite specimen and are directed along and perpendicular to the fibres.

ACKNOWLEDGEMENTS

The authors wish to express their gratitude towards the European Research Office of the U.S. Army for the support and sponsorship as a part of the grant N68171–94–C9108.

REFERENCES

[1] W.J. Bottega, A. Maewal. Delamination buckling and growth in laminates. *Journal of Applied Mechanics*, **50**: 184–189, 1983.

[2] H. Chai, C.D. Babcock, W.G. Knauss. One-dimensional modelling of failure in laminated plates by delamination buckling. *International Journal of Solids and Structures*, **17**: 1069–1083, 1981.

[3] H.P. Chen. Shear deformation theory for compressive delamination buckling and growth. *AIAA Journal*, **29**: 813–819, 1991.

[4] A.L. Kalamkarov. *Composite and reinforced elements of construction.* John Willey and Sons, New York, 1992.

[5] W. Ostachowicz, M. Krawczuk. Dynamic analysis of delaminated composite beam. *Machine Vibration*, **3**: 107–116, 1994.

[6] R.L. Ramkumar, S.V. Kulkarni, R.B. Pipes. Free vibration frequencies of a delaminated beam. *34th Annual Technical Conference Proceedings: Reinforced Composites Institute.* Society of Plastics Industry Inc., 1979.

[7] A. Tessler, S.B. Dong. On a hierarchy of conforming Timoshenko beam elements. *Computers and Structures*, **14**: 335– 344, 1981.

[8] J.R. Vinson, R.L. Sierakowski. *Behaviour of Structures Composed of Composite Materials.* Martinus Nijhoff, Dorchester, 1989.

[9] J.T.S. Wang, Y.Y. Liu, J.A. Gibby. Vibration of split beams. *Journal of Sound and Vibration*, **84**: 491–502, 1982.

[10] J.D. Whitcomb. Parametric analytical study of instability related delamination growth. *Composites Science and Technology*, **25**: 19–46, 1986.

[11] C. Woźniak, M. Woźniak. On the effect of interface micro– cracks on interactions in stratified media. *International Journal of Fracture*, **60**: 165–172, 1994.

[12] C. Woźniak, M. Woźniak. Composite shell with interlaminar imperfections. *Archive of Applied Mechanics*, **63**: 543–550, 1993.

[13] C. Woźniak, M. Woźniak, Z.F. Baczyński. Effect of interlaminar imperfections on a behaviour of laminated plates. *Archive of Applied Mechanics*, **64**: 285–293, 1994.

[14] W.L. Yin, S.N. Sallam, G.J. Simitses. Ultimate axial load capacity of a delaminated beam-plate. *AIAA Journal*, **24**: 123–128, 1986.